7-29-2021

# Laser Irradiation as a Novel Alternative to Detach Intact Particulate Matter Collected on Air Filters

Seyed-Mohammadreza Samaee
*Urmia University, Iran*

Rahim Molaei
*Urmia University, Iran*

Robert A. Yokel
*University of Kentucky*, ryokel@email.uky.edu

Hedieh Pazokian
*Nuclear Science and Technology Research Institute, Iran*

# Laser Irradiation as a Novel Alternative to Detach Intact Particulate Matter Collected on Air Filters

Digital Object Identifier (DOI)
https://doi.org/10.1016/j.chemosphere.2021.131713

Notes/Citation Information
Published in *Chemosphere*, v. 286, part 2, 131713.

# Laser irradiation as a novel alternative to detach intact particulate matter collected on air filters

Seyed-Mohammadreza Samaee[1]*; Rahim Molaei[1], Robert A. Yokel[2], Hedieh Pazokian[3]

[1]Department of Food Hygiene and Quality Control, Faculty of Veterinary Medicine, Urmia University, Urmia 165, Iran;

[2]Department of Pharmaceutical Sciences, University of Kentucky, USA;

[3]Photonics and Quantum Technologies Research School, Nuclear Science and Technology Research Institute, Tehran, Iran

[*]**Corresponding author**: Seyed-Mohammadreza Samaee; **Tel:** +98-044-32770508; **E-mail:** seyedmohammadreza.samaee@gmail.com; **ORCID:** 0000-0002-9104-0299

**Abstract –** Airborne particulate matter (PM) is collected on specific filters. For subsequent testing, the PM should be detached intact from the filter. Liquid extraction (LE), the standard method to detach PM from air filter surfaces, is challenging and can be tedious. Laser irradiation has been used to characterize PM on filters, but not to detach PM from filters for subsequent testing. A feasibility study was conducted to assess the potential of laser irradiation to detach PM from air filters. Laser-detached PM was deposited on a pre-weighed glass plate. PM detachment and collection were conducted in a single step. PM-coated air filters were subjected to visual inspection, gravimetric assessment of captured PM, and spectroscopic scanning (ATR-FTIR, SEM-EDS, and XRD) before and after laser irradiation. Laser irradiation PM detachment efficiency was up to 78%. Functional groups, elements, and minerals of PM collected on filter surfaces disappeared or significantly decreased after irradiation, demonstrating detachment, without suffering a change in their nature. No evidence of filter fragments was found in the detached PM. Laser irradiation was i) an easy, ii) rapid, and iii) single step procedure that iv) detached PM, v) didn't detach filter fragments, vi) didn't change PM composition, and vii) is amenable to automation and high throughput. Laser irradiation to detach PM from air filters as an alternative to LE is worthy of further study and development.

**Keywords:** Air filters, laser irradiation, particulate matter, spectroscopic techniques

## 1. Introduction

Air pollution is a major environmental health issue contributing to up to 7 million premature deaths worldwide annually (Newby et al., 2015; WHO, 2014). Particulate matter (PM), one of the airborne contaminants, presents a major public health concern that contributes

to severe human diseases (Kim et al., 2015) and affects more people than any other air pollutant (WMO, 2015). PM presents far greater complexity than most other common air pollutants that contribute to toxicity (Kelly and Fussell, 2012).

For toxicity testing PM should be i) collected, ii) characterized (physically and chemically), and iii) administered to laboratory animals or cell cultures. Airborne PM is collected on specific filters (e.g. quartz and Teflon). For biological test system exposure, the PM should be detached intact and unchanged from the filter. Liquid-extraction (LE) is the conventional method to detach PM. It is a multistep process involving PM removal from the filter into a solution. There are concerns about LE methods to detach PM from filters; briefly discussed in the following.

Sonication (or vortexing [Kim et al., 2015]) to detach PM can also detach microscopic filter pieces and fragment them into micron-sized sonication-derived filter fragments (SDFF), which can affect biological response (Bein and Wexler, 2014). A standing water sonication suspension (water-SS) does not precipitate the SDFFs (Kim et al., 2015). PM may agglomerate with SDFFs (Bein and Wexler, 2014). SS filtration through gauze (Duan et al., 2017a, 2017b; Du et al., 2017) does not remove SDFFs because gauze does not retain all SDFFs (Bein and Wexler, 2014) and can retain PM. Sonication may not detach PM that has strong cohesive binding to filter fibers or is insufficiently soluble in the extracting medium (Bein and Wexler, 2014). Freeze drying to prepare dry PM can result in significant loss of the organic fraction and dried particles (Bein and Wexler, 2014).

To address the above concerns, Bein and Wexler (2014) suggested a modified LE procedure (multi-solvent extraction [MSE]) in which the water-SS was subjected to filtration through a porous filter membrane to separate it from SDFFs. However, water insoluble PM

exhibited strong cohesive binding to the filter membrane. They were detached by sonication in different solvents followed by filtration to prepare a separate "solvent sonication solution". Organic fraction loss was prevented by liquid-liquid extraction of the "solvent sonication solution" using various solvents to separate "solvent soluble PM fractions". The modifications did not completely address LE shortcomings and added complexity to the methods.

Roper et al. (2019) evaluated six LE methods to extract PM from equal portions of a single filter. They showed that in addition to technical shortcomings, LE impacted the composition and bioactivity of the extracted PM.

Laser ablation is the process of removing material from a surface by irradiating it with a laser beam. It is used in industry (processing and microelectronics), medicine (eye/dental surgery), and cultural heritage (Pouli, 2018). To date laser irradiation to detach PM collected on air filters has only been used as an integral part of destructive analytical methods to characterize PM, such as laser ablation inductively coupled plasma mass spectrometry (ICP-MS) (Tang et al., 2017; Nischkauer et al., 2017; Robinson et al., 2017).

To the authors' knowledge the application of lasers to detach PM from the surface of air filters has not been reported. The current study was a feasibility study to test the hypothesis that laser irradiation has utility to detach PM from air filters while conserving PM properties as they existed on the filter. Spectroscopic analyses were conducted on filters before and after laser irradiation, enabling within filter comparisons.

## 2. Materials and methods

PM (from two collection sites [Supplementary material section S1]) was collected on 53 quartz (Table 1) and seven Teflon (Table S1) filters. The PM-coated filters were weighed,

labeled (section S1), and irradiated with two commonly-available lasers (S2). The PM-coated filters were photographed (Fig. S2), subjected to SEM to determine PM size (S3), gravimetric analysis to determine weight, and spectroscopic scanning (ATR-FTIR [S4], SEM-EDS to determine elemental composition [S5], and X-ray diffraction to identify PM minerals [S6]) before and after laser irradiation. Statistical analyses were performed using IBM SPSS (version 20; SPSS Inc., Chicago, IL, USA). Graphs were drawn using Excel 2010 (Microsoft Corporation, Redmond, WA, USA) (S7).

## 3. Results and discussion

### 3.1. PM detachment success

#### 3.1.1. Visual and electron microscopic evaluation

Visual inspection of PM-coated filters taken before and after laser irradiation provided an initial evaluation of PM detachment. To select photographs for presentation the filters were categorized as low, medium, and high based on their weight before irradiation, as indicated in Tables 1 and S1, then three from each category shown in Fig. S2. Visual inspection shows laser irradiation reduced PM on the filters. SEM micrographs showed a decrease of PM on the filters after KrF irradiation compared to non-irradiated filters (Figs. 1 and S3). Visual and SEM evaluation show PM residues on irradiated filters. This was also seen after LE, attributed to components that are i) water insoluble, ii) small PMs that exhibit strong cohesive binding to filter fibers, and/or iii) maybe lipid soluble (Bein and Wexler, 2014).

#### 3.1.2. Gravimetric analysis

Based on the filter weight after vs. before irradiation, maximum PM detachment efficiency was 72% and 78% for the quartz (Table 1) and Teflon (Table S1) filters, respectively, lower than reported (~ 90%) for the modified LE (Bein and Wexler, 2014, 2015; Roper et al. 2015). This may be the result of selection of a laser fluence below that which would produce filter substrate detachment. Using other lasers, or a combination of lasers, might improve detachment efficiency, providing an opportunity to improve on this study that demonstrated proof of concept.

PM detachment efficiency from the quartz filters significantly and positively correlated with the total PM mass on the filters (Fig. 2A-B). This was not observed for the Teflon filters (Fig. S4A-B). To assess the effect of filter type (Fig. S4C), collection site (Fig. 2C), and collection month (Fig. 2D) on PM detachment efficiency, filters with circa the same total PM mass (3.0-4.8, 4.1-7.0, and 6.1-10 mg) were compared. These factors had no significant effect on detachment efficiency.

3.1.3. PM characterization and detachment

ATR-FTIR, EDS, and XRD spectra peaks from the surface of PM-coated filters before KrF laser irradiation were assigned to PM functional groups (Figs. 3 and S5; Tables 2 and S2), elements (Figs. 4 and S6; Tables 3 and S3), and minerals (Table S4), respectively. Most peaks either disappeared or demonstrated a significant increased ATR-FTIR transmission (Tables 2 and S2) or decreased element and mineral intensity (Tables 3 and S3 for EDS and Table S4 for XRD) after KrF-irradiation.

3.2. Laser advantages in comparison to LEs

142 The laser irradiation method was compared to a LE method, the MSE technique
143 suggested by Bein and Wexler (2014, 2015), as follows.
144
145 3.2.1. Lack of frequent gravimetric analysis and amenability to high throughput
146 In a LE method gravimetric analysis is conducted in at least in ten steps which can
147 compound measurement errors as they propagate through the various calculations. In the laser-
148 based technique used here, PM detachment, collection, and weighing were performed in a single
149 step within 1 h (Section S2). The reduced number of weighing steps decreases this source of
150 measurement error. LEs are multistep (Roper et al., 2015) and time consuming techniques; e.g.
151 the MSE suggested by Bein and Wexler (2014, 2015) is conducted through 66 steps in 5 days
152 while the procedure used herein is performed in a single step, therefore is amenable to
153 automation and high throughput.
154
155 3.2.2. No co-detachment of filter fragments
156 Sonication is a key step in LE, producing micron-sized toxic SDFFs, as an artifact in PM
157 toxicity tests. PM-coated filters were irradiated with a KrF laser at a fluence below the filter
158 substrate detachment threshold. In Fig. 5C the region 1400-400 $cm^{-1}$ shows the predominant
159 peaks of Teflon at 1201, 1146, and 637 $cm^{-1}$. Although the peaks are observed in the ATR-FTIR
160 spectra from the filter surface before and after laser irradiation, they are not in the ATR-FTIR
161 spectra of detached PM. This provides evidence that the laser and laser parameters used did not
162 co-extract filter fragments.
163
164 3.2.3. Intact integrity of detached PM

Roper et al. (2019) evaluated six LE methods to extract PM from equal portions of a single filter. It was found that LE impacts the composition and bioactivity of the extracted PM. This was in agreement with early reports in which the changes in PM composition and structural integrity (Bein and Wexler, 2015, Roper et al. (2015), bioactivity, (Van Winkle et al, 2015), and toxicity (Eiguren-Fernandez et al., 2010; Verma et al., 2012; see also Yang et al., 2014) had been cited.

Comparing various regions (highlighted in Fig. 5A-C) in the ATR-FTIR spectra collected from the surface of PM-coated filters with the spectra of KrF-detached PM, significant qualitative differences were not observed in the peaks. Differences were only related to the decrease in the transmittance of peaks in the filters after irradiation. XRD mineral peak results are shown in the 10 graphs in each of Fig. 5G-I. Comparing XRD of minerals between KrF irradiated (Fig. 5H) and non-irradiated (Fig. 5G) PM-coated filters suggests the KrF laser did not change the nature of PM remaining on the filter. Differences observed between Fig. 5H and Fig. 5G were only related to decreases in peak intensity. In brief, organic compound (Figs. 3 and S5; Tables 2 and S2), element (Figs. 4 and S6; Tables 3 and S3), and mineral (Table S4) results suggest a lack of change in detached PM composition following its detachment.

3.2.4. Recovery of dry PM

To prepare PM for characterization and biological testing, dry PM with a known mass is usually used. Some LE methods use freeze drying to obtain dry PM. During the process part of the PM may be lost (Bein and Wexler, 2014). In the MSE method, Bein and Wexler (2014) cite alternatives to increase the efficiency of the dry PM recovery process although it is not an easy

187 endeavor. The above complications are not observed in laser-based PM detachment in which
188 detached dry PM is directly deposited on pre-weighed glass plates.
189
190 3.2.5. Non-selective detachment
191 The above results show PM deposits remained on the filters after KrF irradiation.
192 Remaining PM residues have also been cited in LE methods after $H_2O$ sonication of filters. Bein
193 and Wexler (2014) attributed the residues to components that i) are $H_2O$ insoluble, ii) exhibit
194 strong cohesive binding to filter fibers, and/or iii) are maybe lipid soluble. In the current study,
195 PM characterization after compared to before KrF irradiation using ATR-FTIR [Figs. 3 and S5],
196 SEM-EDS [Figs. 4 and S6], and XRD [Table S4] demonstrated similar profiles of functional
197 groups, elements, and minerals, i.e. the laser non-selectively ablated PM, regardless of PM
198 chemical composition. It is assumed that the non-detached residues on the filters in the present
199 study are small PMs (Fig. 1 E, J, O, T, Y, AD) that have strong cohesive binding to the filter's
200 substrate.
201
202 3.3. Assessment of a second laser
203 In 3.1.2 the use of other lasers, or a combination of lasers, is suggested as an alternative
204 to increase laser irradiation-induced detachment efficiency. As a preliminary endeavor the PM
205 detachment process was repeated using another available laser, Nd:YAG.
206 For this assessment, equal portions of PM-coated filters were irradiated with KrF and
207 Nd:YAG lasers and compared to each other and to a non-irradiated portion of the same filter.
208 ATR-FTIR (Fig. 5A-F), and XRD (Fig. 5G-I) were conducted before and after irradiation.

ATR-FTIR spectra from the KrF laser detached PM (Fig. 5A-C) was more similar to the spectra collected from the surface of the PM-coated filter before laser irradiation than PM detached by the Nd:YAG laser (Fig. 5D-F), indicating better detachment of intact particulates by KrF laser irradiation.

After KrF laser irradiation the XRD intensity of particulate components on the PM-coated filter was considerably less, indicated by the lower Y scale range of Fig. 5H compared to the non-irradiated filter (Fig. 5G). In contrast, there was little difference in XRD intensity of particulates on the filter after Nd:YAG irradiation (Fig. 5I) compared to the non-irradiated filter (Fig. 5G). These results show the KrF laser more effectively detached PM minerals than the Nd:YAG laser.

Comparing ATR-FTIR and XRD spectra after KrF laser irradiation (Fig. 5A-C and Fig. 5H) and after Nd:YAG laser irradiation (Fig. 5D-F and Fig. 5I) to non-irradiated PM-coated filters (Fig. 5A-F and 5G) showed neither laser changed the nature of PM that remained on the filter.

## 4. Conclusion

This proof of concept study demonstrated 1) Laser irradiation has the potential to detach PM from the surface of air filters, 2) Detachment efficiency up to 78% was achieved, 3) Detachment efficiency was not filter type, collection site, or collection month dependent, 4) Laser irradiation quantitatively reduced PM functional groups, elements, and compounds without qualitative change, and 5) Laser irradiation did not co-detach filter substrate. Laser-based PM detachment was an easy and rapid alternative to LE methods to detach PM collected on air filters, amenable to automation and high throughput. There are limitations to this feasibility

study: a) A lower detachment efficiency was obtained than reported for MSE. b) There was a significant relationship between detachment efficiency and total PM mass on quartz filters. A different or a series of lasers might abrogate these relationships. The preliminary results obtained in the current study warrant follow-up with further study.

## Declaration of Competing Interest

All authors declare no conflict of interest.


## Acknowledgement

The authors would like to thank Dr. Hesam Ahmady-Birgani (Urmia University, Iran) for donation of the PM filters used in the current research.


## Supplementary material

The Supplementary material is available free of charge at:

https://.

## Author contributions

**Seyed-Mohammadreza Samaee:** Conceptualization, Writing - original draft, Methodology, Validation, Visualization, Formal analysis, Supervision, Data curation, and Funding. **Rahim Molaei:** Formal analysis. **Robert A. Yokel:** Writing – critical review & editing (both scientific and linguistic). **Hedieh Pazokian:** Laser irradiation of filters.

## References

Bein, K.J., Wexler, A.S., 2014. A high-efficiency, low-bias method for extracting particulate matter from filter and impactor substrates. Atmos. Environ. 90, 87-95. https://doi.org/10.1016/j.atmosenv.2014.03.042.

Bein, K.J., Wexler, A.S., 2015. Compositional variance in extracted particulate matter using different filter extraction techniques. Atmos. Environ. 107, 24–34. https://doi.org/10.1016/j.atmosenv.2015.02.026.

Du, X., Jiang, S., Bo, L., Liu, J., Zeng, X., Xie, Y., He, Q., Ye, X., Song, W., Zhao, J., 2017. Combined effects of vitamin E and omega-3 fatty acids on protecting ambient PM2.5-induced cardiovascular injury in rats. Chemosphere 173, 14-21. https://doi: 10.1016/j.chemosphere.2017.01.042.

Duan, J., Hu, H., Zhang, Y., Feng, L., Shi, Y., Miller, M.R., Sun. Z., 2017a. Multi-organ toxicity induced by fine particulate matter $PM_{2.5}$ in zebrafish (*Danio rerio*) model. Chemosphere 180: 24–32. https://doi: 10.1016/j.chemosphere.2017.04.013.

Duan, J., Yu, Y., Li, Y., Jing, L., Yang, M., Wang, J., Li, Y., Zhou, X., Miller, M.R., Sun, Z., 2017b. Comprehensive understanding of $PM_{2.5}$ on gene and microRNA expression patterns in zebrafish (*Danio rerio*) model. Sci. Total Environ. 586, 666–674. https://doi: 10.1016/j.scitotenv.2017.02.042.

Eiguren-Fernandez A, Shinyashiki M, Schmitz DA, DiStefano E, Hinds W, Kumagai Y, Cho AK, Froines JR. 2010. Redox and electrophilic properties of vapor- and particle-phase components of ambient aerosols. Environ Res 110:207–212.

Jeong, S.C., Song, M.K., Cho, Y., Lee, E., Ryu, J.C., 2017. Integrative analysis of mRNA and microRNA expression of a human alveolar epithelial cell (A549) exposed to water and

organic-soluble extract from particulate matter $(PM)_{2.5}$. Environ. Toxicol. 32, 302–310. https://doi: 10.1002/tox.22236.

Kelly, F.J., Fussell, J.C., 2012. Size, source and chemical composition as determinants of toxicity attributable to ambient particulate matter. Atmos. Environ. 60, 504–526. https://doi.org/10.1016/j.atmosenv.2012.06.039.

Kim, J.Y., Lee, E.Y., Choi, I., Kim, J., Cho, K.H., 2015. Effects of the particulate matter 2.5 ($PM_{2.5}$) on lipoprotein metabolism, uptake and degradation, and embryo toxicity. Mol. Cells 38, 1096–1104. https://doi.org/10.14348/molcells.2015.0194.

Newby, D.E., Mannucci, P.M., Tell, G.S., Baccarelli, A.A., Brook, R.D., Donaldson, K., Forastiere, F., Franchini, M., Franco, O.H., Graham, I., Hoek, G., Hoffmann, B., Hoylaerts, M.F., Kunzli, N., Mills, N., Pekkanen, J., Peters, A., Piepoli, M.F., Rajagopalan, S., Storey, R.F., 2015. Expert position paper on air pollution and cardiovascular disease. Eur. Heart J. 36, 83−93. https://doi.org/10.1093/eurheartj/ehu458.

Nischkauer, W., Izmer, A., Neouze, M-.A., Vanhaecke, F., Limbeck, A. 2017. Combining Dispersed Particle Extraction with Dried-Droplet Laser Ablation ICP-MS for Determining Platinum in Airborne Particulate Matter. Appl. Spectrosc. 71(7), 1613−1620.

Pouli, P., 2018. Laser Cleaning. The Encyclopedia of Archaeological Sciences, López Varela, S.L., Eds; John Wiley & Sons, Inc. 1-4. https://doi.org/10.1002/9781119188230.saseas0341.

Robinson, M.S., Grgić, I., Šelih, V.S., Šala, M., Bitsui, M., van Elteren, J.T. 2017. Laser ablation ICP-MS of size-segregated atmospheric particles collected with a MOUDI cascade impactor: a proof of concept. Atmos. Meas. Tech. 10, 1823−1830.

Roper, C., Chubb, L.G., Cambal, L., Tunno, B., Clougherty, J.E., Mischler, S.E., 2015. Characterization of ambient and extracted PM2.5 collected on filters for toxicology applications. Inhal. Toxicol. 27, 673–681. https://doi.org/10.3109/08958378.2015.1092185.

Roper, C., Delgado, L.S., Barrett, D., Simonich, S.L.M., Tanguay, R.L., 2019. $PM_{2.5}$ filter extraction methods: Implications for chemical and toxicological analyses. Environ. Sci. Technol. 53, 434−442. https://doi.org/10.1021/acs.est.8b04308.

Tang, X., Qian, Y., Guo, Y., Wei, N., Li, Y., Yao, J., Wang, G., Ma, J., Liu, W. 2017. Analysis of atmospheric pollutant metals by laser ablation inductively coupled plasma mass spectrometry with a radial line-scan dried-droplet approach. Spectrochim. Acta. B. 138, 18–22.

Van Winkle LS, Bein K, Anderson D, Pinkerton KE, Tablin F, Wilson D, Wexler AS. 2015. Biological dose response to $PM_{2.5}$: effect of particle extraction method on platelet and lung responses. Toxicol Sci 143:349–59.

Verma V, Rico-Martinez R, Kotra N, King L, Liu J, Snell TW, Weber RJ. 2012. Contribution of water-soluble and insoluble components and their hydrophobic/ hydrophilic subfractions to the reactive oxygen species-generating potential of fine ambient aerosols. Environ. Sci Technol 46:11384–11392.

World Health Organization (WHO). 2014. 7 million premature deaths annually linked to air pollution. http://www.who.int/mediacentre/news/releases/2014/air-pollution/en/ (accessed on 23-09-2020).

World Meteorological Organization (WMO). 2015. Health Impacts of Airborne Dust. https://public.wmo.int/en/resources/meteoworld/health-impacts-of-airborne-dust (accessed on 23-09-2020).

**Fig. 1.** SEM images of PM-coated quartz filters before (A through AB indicated by [b]) and after (B through AC indicated by [a]) KrF laser irradiation. AE is a non-PM exposed quartz filter.

Figures in the right-hand column show the size distribution of PM collected on the filters. See Table 1 for the filter identities.

**Fig. 2.** Weight of 53 PM-coated air filters and PM detachment efficiency. (A) Weight of PM-coated quartz filters before and after laser irradiation. (B) PM mass deposited on filters in relation to PM detachment efficiency. (C) The effect of PM collection site. (D) The effect of collection month on PM detachment efficiency. See Table 1 for the filter code identities.

**Fig. 3.** ATR-FTIR of PM-coated quartz filters before and after KrF laser irradiation. See Table 1 for the filter code identities.

**Fig. 4.** EDS of PM-coated quartz filters before and after KrF laser irradiation and blank (Y). The inserted images show a field of view with the particle of interest. [b]: before laser irradiation; [a]: after laser irradiation. The white arrows point out analyzed particles. See Table 1 for the filter identities.

**Fig. 5.** Laser irradiation-induced PM detachment from filters and filter damage. (A-C) ATR-FTIR spectra from the surface of a PM-coated Teflon filter before and after KrF irradiation and the detached PM. (D-F) ATR-FTIR spectra before and after Nd:YAG irradiation and the detached PM. (G-I) XRD spectra from the surface of a PM-coated Teflon filter before (G) and after (KrF [H] and Nd:YAG [I]]) irradiation. KAO: kaolinite, CLI: clinochlore, PHI: phillipsite, ILL: illite, MAS: mascagnite, KOK: koktaite, QUA: quartz, BEI: beidellite, RUT: rutile, and GYP: gypsum.

**Table 1.** PM-coated quartz filters analyzed in this study.

| No. | Site | Collection Date | Code | Filter weight (mg) | | Detachment efficiency (%) |
|---|---|---|---|---|---|---|
| | | | | before irradiation | after irradiation | |
| 1 | UU | 2017-02-19 | F-49 | 1.70 | 1.60 | 5.90 |
| 2 | UU | 2017-02-23 | F-50 | 1.20 | 1.06 | 11.67 |
| 3 | UU | 2017-02-28 | F-47 | *2.04* | 1.50 | 26.47 |
| 4 | UU | 2017-03-05 | F-5 | **7.00** | 3.15 | 55.00 |
| 5 | UU | 2016-05-21 | F-24 | 1.00 | 0.96 | 4.00 |
| 6 | UU | 2016-05-25 | F-30 | 0.80 | 0.77 | 3.75 |
| 7 | UU | 2016-05-30 | F-27 | 1.33 | 1.23 | 7.51 |
| 8 | UU | 2016-06-04 | F-28 | *2.88* | 2.11 | 26.74 |
| 9 | UU | 2016-06-09 | F-29 | **3.86** | 2.33 | 39.64 |
| 10 | UU | 2016-06-14 | F-25 | 0.60 | 0.58 | 3.33 |
| 11 | UU | 2016-06-21 | F-26 | **4.12** | 2.63 | 36.17 |
| 12 | UU | 2016-06-25 | F-2 | 1.22 | 1.11 | 9.02 |
| 13 | UU | 2016-06-30 | F-31 | **4.24** | 2.34 | 44.81 |
| 14 | UU | 2016-07-05 | F-23 | *1.87* | 1.37 | 26.74 |
| 15 | UU | 2016-07-10 | F-22 | 1.33 | 1.16 | 12.78 |
| 16 | UU | 2016-07-15 | F-7 | **11.87** | 4.81 | 59.48 |
| 17 | UU | 2016-10-22 | F-34 | **15.41** | 4.3 | 72.10 |
| 18 | UU | 2016-10-26 | F-32 | *1.61* | 1.35 | 16.15 |
| 19 | UU | 2016-10-31 | F-33 | *1.77* | 1.31 | 25.99 |
| 20 | UU | 2016-11-05 | F-21 | *1.78* | 1.32 | 25.84 |
| 21 | UU | 2016-11-10 | F-1 | **7.03** | 2.8 | 60.17 |
| 22 | UU | 2017-10-23 | F-10 | **14.27** | 5.71 | 59.99 |
| 23 | UU | 2018-01-21 | F-12 | *1.64* | 1.32 | 19.51 |
| 24 | RD | 2016-09-22 | F-60 | 1.64 | 1.58 | 3.66 |
| 25 | RD | 2016-09-26 | F-61 | 0.92 | 0.89 | 3.26 |
| 26 | RD | 2016-10-01 | F-59 | **4.39** | 2.66 | 39.41 |
| 27 | RD | 2016-10-22 | F-51 | 2.03 | 1.83 | 9.85 |
| 28 | RD | 2016-10-26 | F-56 | **6.96** | 2.83 | 59.34 |
| 29 | RD | 2016-10-31 | F-52 | **4.34** | 3.08 | 29.03 |
| 30 | RD | 2016-11-05 | F-58 | **4.48** | 2.92 | 34.82 |
| 31 | RD | 2016-11-10 | F-53 | **6.14** | 3.35 | 45.44 |
| 32 | RD | 2016-11-10 | F-54 | **6.36** | 3.03 | 52.36 |
| 33 | RD | 2016-11-21 | F-57 | 1.85 | 1.7 | 8.11 |
| 34 | RD | 2016-11-25 | F-55 | 1.15 | 1.11 | 3.48 |
| 35 | RD | 2017-02-19 | F-46 | 2.02 | 1.81 | 10.40 |
| 36 | RD | 2017-02-23 | F-40 | *4.14* | 3.1 | 25.12 |
| 37 | RD | 2017-01-20 | F-11 | *3.04* | 2.51 | 17.43 |
| 38 | RD | 2017-01-24 | F-41 | *3.43* | 2.75 | 19.83 |
| 39 | RD | 2017-01-29 | F-38 | *4.06* | 3.17 | 21.92 |
| 40 | RD | 2017-02-03 | F-48 | *2.87* | 2.40 | 16.38 |
| 41 | RD | 2017-03-21 | F-43 | 0.84 | 0.82 | 2.38 |
| 42 | RD | 2017-03-25 | F-37 | *2.74* | 2.31 | 15.69 |
| 43 | RD | 2017-03-30 | F-35 | 2.43 | 2.13 | 12.35 |
| 44 | RD | 2017-04-04 | F-36 | *2.73* | 2.33 | 14.65 |
| 45 | RD | 2017-04-21 | F-39 | *2.56* | 2.28 | 10.94 |
| 46 | RD | 2017-04-25 | F-44 | **2.76** | 2.31 | 16.30 |
| 47 | RD | 2017-04-30 | F-4 | **4.52** | 2.87 | 36.50 |
| 48 | RD | 2017-05-22 | F-45 | 1.23 | 1.17 | 4.88 |
| 49 | RD | 2017-08-23 | F-42 | *3.09* | 2.5 | 19.09 |
| 50 | RD | 2017-11-22 | F-3 | **4.39** | 3.00 | 31.66 |
| 51 | RD | 2017-11-26 | F-16 | *3.30* | 2.69 | 18.48 |
| 52 | RD | 2018-01-21 | F-13 | 1.15 | 1.07 | 6.96 |
| 53 | RD | 2018-02-20 | F-15 | *4.01* | 3.2 | 20.20 |

UU: Urmia University; RD: Rashkan district; Low weight PM-coated filters are underlined; medium are in italic; high are in boldface.

**Table 2.** Peak intensity of ATR-FTIR spectra functional groups collected from quartz filter surfaces before (B) and after (A) KrF irradiation.

| Peaks | Functional groups related to the peaks | Peak intensity of PM-coated quartz filters | | | |
|---|---|---|---|---|---|
| | | UU (Table 1, rows 1-23) | | RD (Table 1, rows 24-53) | |
| | | B-KrF | A-KrF | B-KrF | A-KrF |
| 3530-3224 | O-H, N-H | 91.0 ± 2.0 | 97.4 ± 0.7* | 92.6 ± 3.9 | 98.3 ± 1.3* |
| 3063-3040 | Si – CH = $CH_2$ | 97.7 ± 0.0 | 99.0 ± 0.0* | 95.0 ± 0.8 | 97.8 ± 0.2* |
| 2918 | Methyl | 97.5 ± 0.7 | 97.9 ± 1.8 | 96.8 ± 1.2 | 99.1 ± 0.4* |
| 2850 | Methylene | 98.4 ± 0.2 | 98.9 ± 0.3 | 97.2 ± 1.8 | 99.1 ± 0.1 |
| 1625-1615 | Organonitrates, ammonium and its salts | 87.3 ± 7.2 | 96.2 ± 0.7 | 86.3 ± 12.8 | 97.5 ± 1.3 |
| 1450-1400 | Organonitrates, ammonium and its salts | 82.6 ± 8.6 | 92.7 ± 3.8 | 75.1 ± 11.7 | 92.0 ± 5.5* |
| 1142-1096 | Sulfate groups | 71.9 ± 10.4 | 82.3 ± 14.8 | 69.7 ± 16.4 | 90.4 ± 2.8 |
| 1034-909 | Si-O-Si symmetrical stretching vibration | 43.9 ± 24.8 | 62.6 ± 19.4 | 48.4 ± 17.7 | 71.0 ± 10.7 |
| 875-821 | Nitrate | 63.4 ± 26.2 | 75.0 ± 24.4 | 73.6 ± 16.5 | 91.8 ± 5.0 |
| 670-610 | Sulfate groups | 69.6 ± 16.0 | 80.4 ± 19.5 | 74.1 ± 17.1 | 92.1 ± 2.8 |
| 445-414 | Si–O asymmetrical bending vibration | 79.6 ± 6.3 | 84.3 ± 6.0 | 65.2 ± 16.9 | 74.1 ± 10.7 |

* indicates functional groups that underwent a significant quantitative decrease (increased transmission) after irradiation. UU: Urmia University; RD: Rashkan district

**Table 3.** Energy dispersive spectroscopy (EDS) peak intensity of elements collected from quartz filter surfaces before (B) and after (A) KrF irradiation.

| Peaks | EDS peak intensity of PM-coated quartz filters | | | |
|---|---|---|---|---|
| | UU (Table 1, rows 1-23) | | RD (Table 1, rows 24-53) | |
| | B-KrF | A-KrF | B-KrF | A-KrF |
| **C** | 27.4 ± 11.6 | 13.2 ± 8.3* | 94.0 ± 65.9 | 52.2 ± 55.4 |
| **O** | 305.7 ± 102.0 | 201.3 ± 39.6* | 343.9 ± 76.0 | 270.0 ± 76.5 |
| **Na** | 19.2 ± 13.7 | 1.0 ± 1.5* | 8.7 ± 3.7 | 3.4 ± 5.2 |
| **Mg** | 46.9 ± 30.5 | 7.9 ± 4.6* | 37.4 ± 28.3 | 11.2 ± 4.8* |
| **Al** | 197.4 ± 57.7 | 57.7 ± 33.6* | 90.8 ± 46.4 | 69.7 ± 73.7 |
| **Si** | 737.2 ± 141.7 | 688.8 ± 146.0 | 692.3 ± 160.4 | 849.0 ± 97.8 |
| **S** | 34.1 ± 14.6 | 71.8 ± 31.7 | 73.9 ± 86.0 | 37.7 ± 15.9 |
| **Cl** | 13.0 ± 7.8 | 5.3 ± 8.8 | 7.8 ± 1.1 | 4.5 ± 1.8 |
| **K** | 41.3 ± 22.3 | 11.2 ± 7.0* | 26.6 ± 9.6 | 13.7 ± 17.4 |
| **Ca** | 64.5 ± 45.8 | 74.6 ± 67.1 | 70.6 ± 57.5 | 18.5 ± 21.5* |
| **Ti** | 4.3 ± 0.8 | 2.3 ± 3.2 | – | – |
| **Fe** | 22.2 ± 12.3 | 6.0 ± 4.3* | 18.2 ± 13.2 | 8.1 ± 7.4 |
| **Zn** | – | – | – | – |
| **F** | – | – | – | – |

* indicates elements that underwent a significant quantitative decrease after irradiation. UU: Urmia University; RD: Rashkan district

387 Figure 1

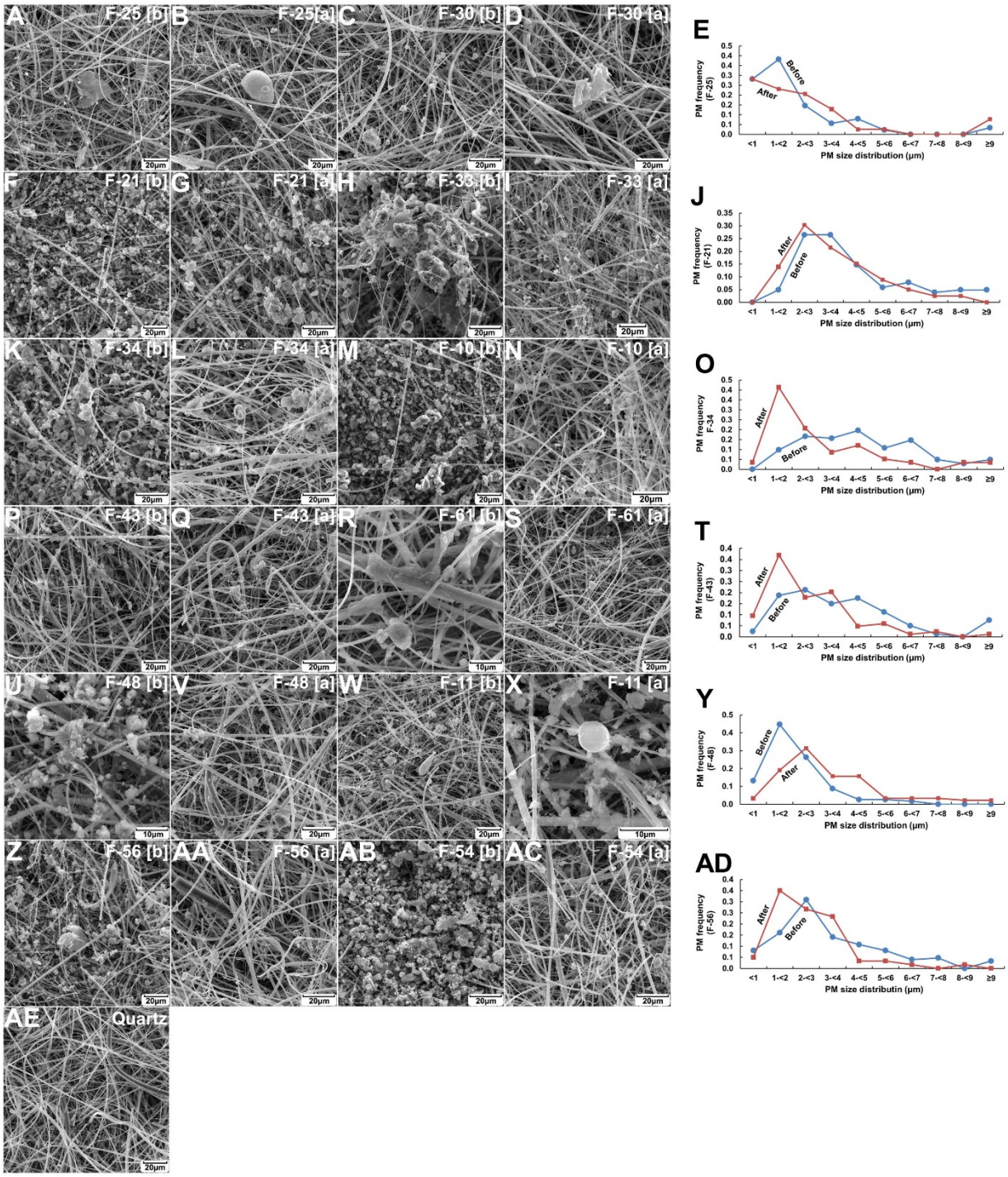


388

389

390 Figure 2

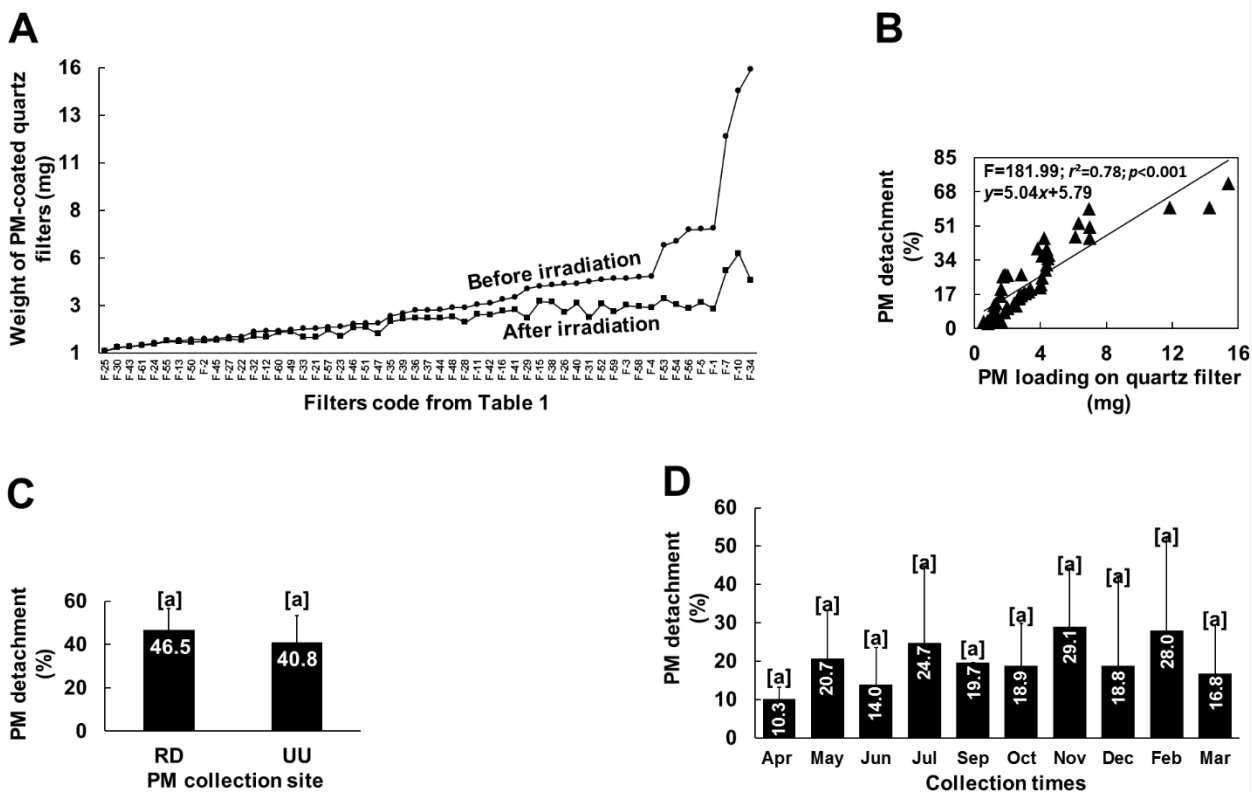


391

392

393 Figure 3

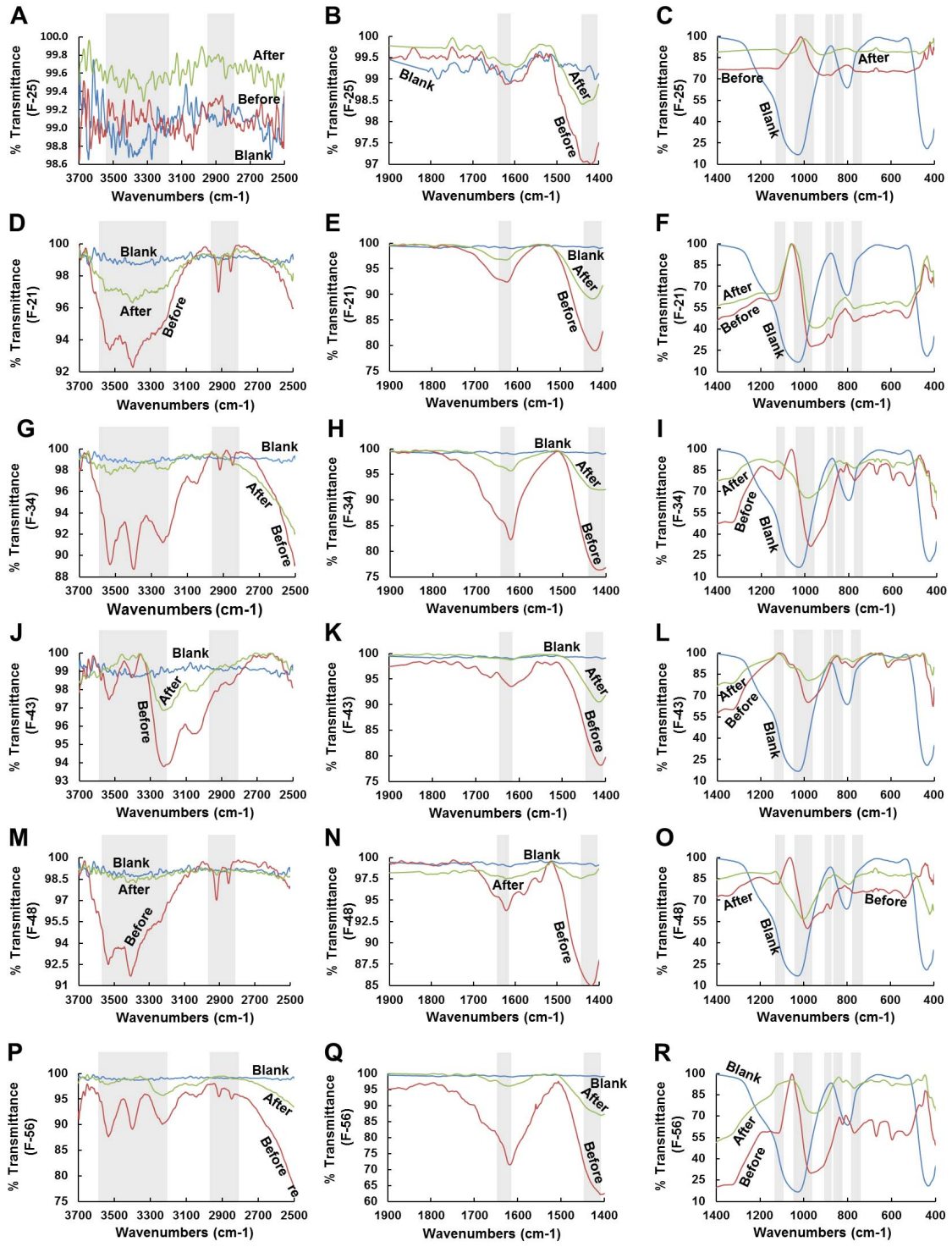


394

395

Figure 4

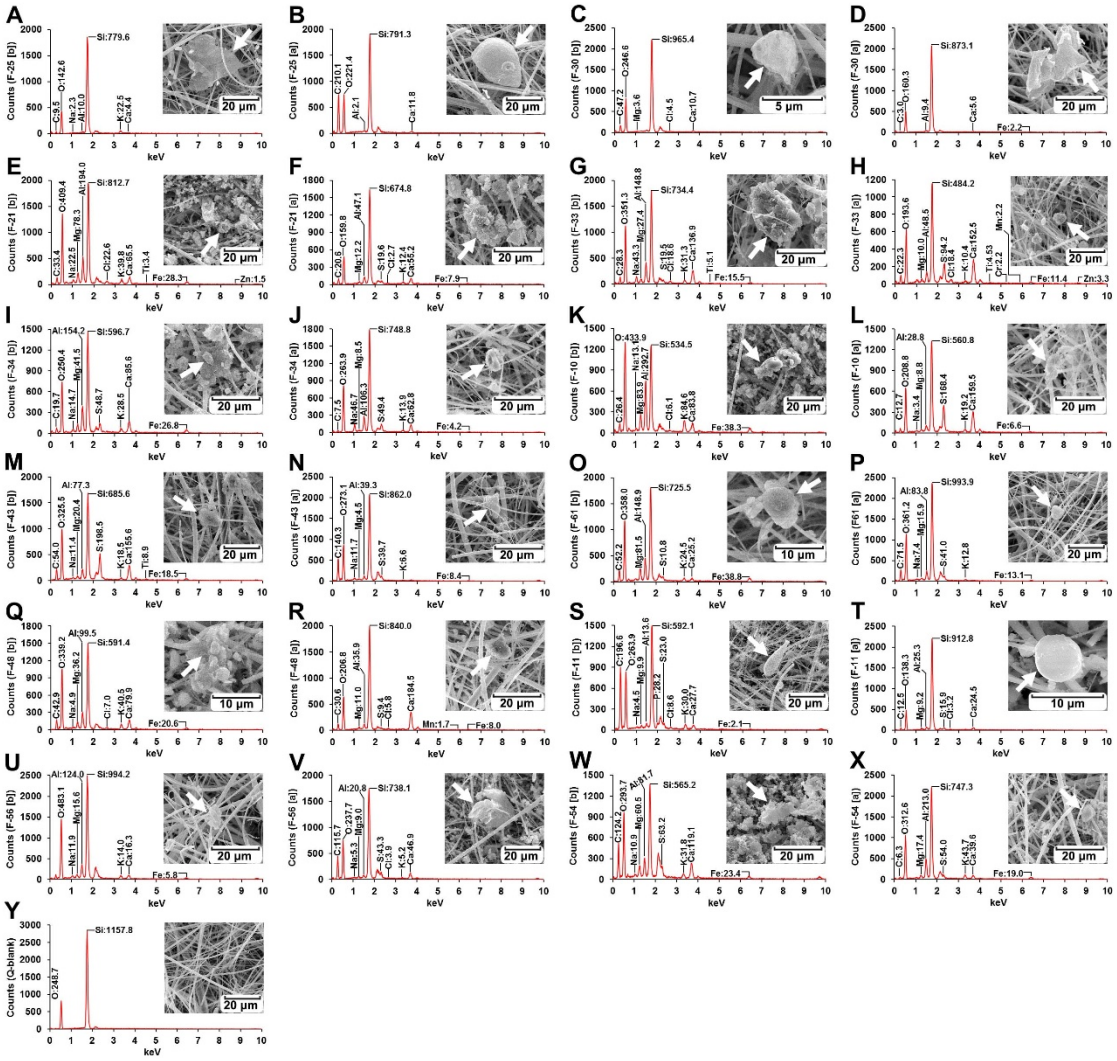
A
Counts (F-25 [b])
Si:779.6
20 μm
B
Counts (F-25 [a])
Si:791.3
20 μm
C
Counts (F-30 [b])
Si:965.4
5 μm
D
Counts (F-30 [a])
Si:873.1
20 μm
E
Counts (F-21 [b])
Si:812.7
20 μm
F
Counts (F-21 [a])
Si:674.8
20 μm
G
Counts (F-33 [b])
Si:734.4
20 μm
H
Counts (F-33 [a])
Si:484.2
20 μm
I
Counts (F-34 [b])
Al:154.2
Si:596.7
20 μm
J
Counts (F-34 [a])
Si:748.8
20 μm
K
Counts (F-10 [b])
Si:534.5
20 μm
L
Counts (F-10 [a])
Si:560.8
20 μm
M
Counts (F-43 [b])
Al:77.3
Si:685.6
20 μm
N
Counts (F-43 [a])
Al:39.3
Si:862.0
20 μm
O
Counts (F-61 [b])
Si:725.5
10 μm
P
Counts (F61 [a])
Al:83.8
Si:993.9
20 μm
Q
Counts (F-48 [b])
Al:99.5
Si:591.4
10 μm
R
Counts (F-48 [a])
Si:840.0
20 μm
S
Counts (F-11 [b])
Si:592.1
20 μm
T
Counts (F-11 [a])
Si:912.8
10 μm
U
Counts (F-55 [b])
Al:124.0
Si:994.2
20 μm
V
Counts (F-55 [a])
Al:20.8
Si:738.1
20 μm
W
Counts (F-54 [b])
Si:565.2
20 μm
X
Counts (F-54 [a])
Si:747.3
20 μm
Y
Counts (Q-blank)
Si:1157.8
20 μm
keV

399 Figure 5

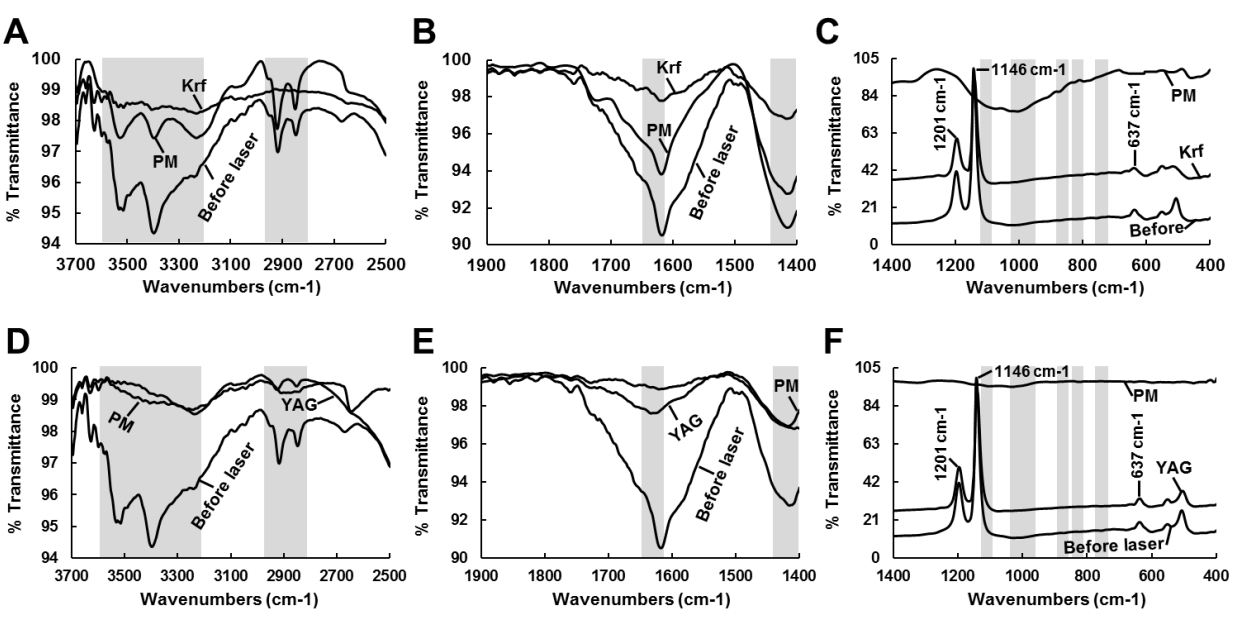


400

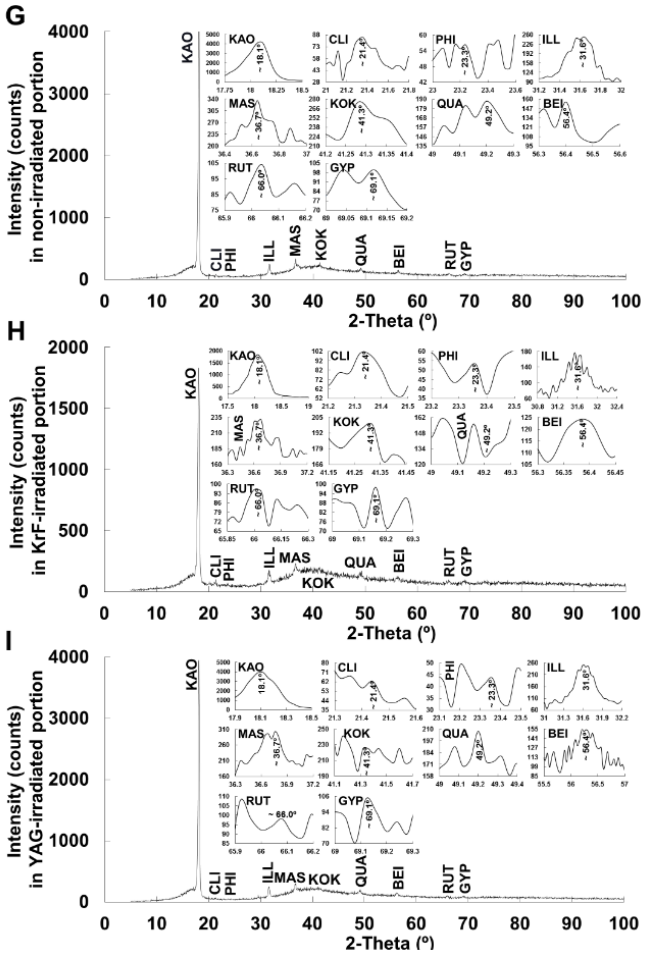


401

Supplementary material

# Laser irradiation as a novel alternative to detach intact particulate matter collected on air filters

Seyed-Mohammadreza Samaee[1]*; Rahim Molaei[1], Robert A. Yokel[2], Hedieh Pazokian[3]

[1]Department of Food Hygiene and Quality Control, Faculty of Veterinary Medicine, Urmia University, Urmia 165, Iran;

[2]Department of Pharmaceutical Sciences, University of Kentucky, USA;

[3]Photonics and Quantum Technologies Research School, Nuclear Science and Technology Research Institute, Tehran, Iran

*Corresponding author: Seyed-Mohammadreza Samaee;

**E-mail address:** seyedmohammadreza.samaee@gmail.com;

**ORCID:** 0000-0002-9104-0299

## S Methods

**S1** PM collection and handling

A study conducted in the Urmia University, Iran by colleagues has two PM collection sites: 1) Urmia University (UU), on the roof top of the Faculty of Natural Resources building, ~ 6 m above ground, (Nazlu district, 11 km from an urban area), and 2) Rashkan district (RD) (near Urmia Lake, ~ 6 m above ground). PM was collected on pre-weighed quartz (Micro-Quartz Fiber Paper, 50 mm diameter, Munktell/Ahlstrom, Sweden) and Teflon (50 mm diameter, Sartorius Stedim Biotech, Germany) filters by a Medium Volume Sampler (Comde-Derenda, Germany) equipped with a $PM_{10}$ inlet. Each filter was i) weighed before and after exposure to determine PM mass to $10^{-4}$ g, ii) photographed (Sony Xperia TX 13 MP camera, Japan) for a visual inspection of PM coating, iii) cut into four pieces using ethanol (70%) prewashed scissors, one piece subjected to PM characterization using spectroscopic techniques, two laser irradiated, and one archived, iv) packed into a zipper plastic bag labelled with the collection site, time, and date, and v) stored at 4 °C to prevent microorganism growth and chemical alteration.

**S2** Laser techniques

PM was detached by a 30 ns KrF laser (248 nm) and the second harmonic of a Q-switch Nd:YAG laser (8 ns, 532 nm). They were utilized because of their availability and the ease of selection of a transparent substrate (glass) for detached PM collection. The laser beam, after passing through a 23 cm diameter aperture, was reflected from a flat mirror at 45º and focused onto the filter by a 10 cm focal length lens. A pre-weighed glass plate was placed on the PM-coated filter in contact with the filter surface. The laser beam passed through the glass plate. The detached PM "rose" onto the glass plate. The filter was mounted on an *x-y* table driven by a stepping motor which enabled table movement at a defined speed. The filter samples were

irradiated with a scanning velocity of 1 mm/s with pulse repetition rate of 1 Hz. Laser fluence is the most important parameter for PM detachment. Laser induced material detachment occurs at the threshold fluence. Laser fluence was set to a value to avoid filter damage yet detach PM.

**S3** PM size distribution

A scanning electron microscope (SEM) (VEGA3 TESCAN) was used to evaluate the size of PM deposited on filters. Electron micrographs were taken from two fields on each filter. The size of 100 particulates on the micrographs of each filter was determined using Image J (Ver 1.48).

**S4** PM organic matter composition

ATR-FTIR was carried out to collect PM organic matter spectra in transmittance mode with a resolution of 4 $cm^{-1}$ by a Thermo Nicolet Nexus 870 spectrophotometer using Smart Orbit Diamond ATR in the region 400 to 4000 $cm^{-1}$. Omnic Software (Ver 6; Thermo Nicolet) was used to analyze the ATR-spectra. Spectral changes were explored in three distinct zones: single bond stretch (2500-3700 $cm^{-1}$), double bond stretch (1400-1900 $cm^{-1}$), and the fingerprint region (400-1400 $cm^{-1}$).

**S5** PM elemental composition

Energy dispersive spectroscopy (EDS) (Sirius-SD, UK) was used to evaluate PM elemental composition.

**S6** PM minerals

To identify PM minerals, a small piece of PM-coated filter was placed on a holding plate, inserted into a X-ray diffractometer (Rigaku ULTIMA IV, Japan), and scanned from 1º to 90º 2θ at 1º per min. PM mineral peaks were manually analyzed by Highscore Plus software (Ver 3.06 [3.0.5]; PANalytical B.V. Almelo, The Netherlands).

**S7** Statistical analysis

Values are reported as mean ± S.D. Differences between groups were evaluated by *t*-tests. A *p*-value of 0.05 was used to accept statistical significance. Simple regression models were formulated between PM loading on filters and PM-detachment efficiency. Significance levels for the regression analyses were selected after applying the Bonferroni's adjustment. All analyses were performed using IBM SPSS (version 20; SPSS Inc., Chicago, IL, USA), and Excel 2010 (Microsoft Corporation, Redmond, WA, USA).

**Table S1.** PM-coated Teflon filters analyzed in this study.

| No. | Site | Collection Date | Code | Type | Filter weight (mg) | | Detachment efficiency (%) |
|---|---|---|---|---|---|---|---|
| | | | | | before irradiation | after irradiation | |
| 1 | RD | 2017-12-16 | F-20 | T | <u>6.37</u> | 1.41 | 77.80 |
| 2 | UU | 2017-12-01 | F-17 | T | <u>6.27</u> | 2.67 | 57.42 |
| 3 | RD | 2017-12-11 | F-19 | T | *6.96* | 2.96 | 57.47 |
| 4 | UU | 2017-12-26 | F-9 | T | *7.41* | 3.55 | 52.10 |
| 5 | UU | 2017-12-22 | F-6 | T | *8.29* | 3.49 | 57.90 |
| 6 | UU | 2017-12-06 | F-18 | T | **9.36** | 4.86 | 48.08 |
| 7 | UU | 2018-02-24 | F-14 | T | **9.92** | 4.52 | 54.44 |

UU: Urmia University; RD: Rashkan district; Low weight PM-coated filters are underlined; medium are in italic; high are in boldface.

**Table S2.** Peak intensity of ATR-FTIR spectra functional groups collected from Teflon filter surfaces before (B) and after (A) KrF irradiation.

| **Peaks** | **Functional groups related to the peaks** | **Peak intensity PM-coated T filters** (Table S1) | |
|---|---|---|---|
| | | B-KrF | A-KrF |
| 3530-3224 | O-H, N-H | 95.3 ± 3.3 | 97.8 ± 2.1 |
| 3063-3040 | Si – CH = $CH_2$ | 94.6 ± 3.6 | 96.8 ± 1.9 |
| 2918 | Methyl | 95.6 ± 1.0 | 98.6 ± 1.0* |
| 2850 | Methylene | 96.6 ± 0.9 | 98.7 ± 0.8* |
| 1625-1615 | Organonitrates, ammonium and its salts | 93.4 ± 4.4 | 99.1 ± 0.8* |
| 1450-1400 | Organonitrates, ammonium and its salts | 62.6 ± 4.2 | 90.1 ± 5.6* |
| 1142-1096 | Sulfate groups | – | – |
| 1034-909 | Si-O-Si symmetrical stretching vibration | 32.4 ± 19.8 | 75.3 ± 31.1 |
| 875-821 | Nitrate | 44.1 ± 16.3 | 79.8 ± 20.6* |
| 670-610 | Sulfate groups | 43.3 ± 16.7 | 77.2 ± 20.9* |
| 445-414 | Si–O asymmetrical bending vibration | 40.7 ± 18.2 | 73.7 ± 21.4 |

* indicates functional groups that their peaks underwent a significant quantitative decrease (increased transmission) after irradiation.

**Table S3.** Energy dispersive spectroscopy (EDS) peak intensity of elements collected from Teflon filter surfaces before (B) and after (A) KrF irradiation.

| Peaks | EDS peak intensity of PM-coated T filters | |
|---|---|---|
| | B-KrF | A-KrF |
| **C** | 109.4 ± 156.5 | 108.4 ± 89.2 |
| **O** | 164.3 ± 64.4 | 70.1 ± 47.8* |
| **Na** | 58.3 ± 74.6 | 6.8 ± 2.4 |
| **Mg** | 11.6 ± 3.0 | 2.4 ± 4.9* |
| **Al** | 47.6 ± 43.2 | 2.6 ± 6.4* |
| **Si** | 97.6 ± 61.3 | 20.1 ± 26.1* |
| **S** | 126.5 ± 125.9 | 96.6 ± 103.7 |
| **Cl** | 9.3 ± 9.1 | 19.9 ± 21.2 |
| **K** | 28.4 ± 24.7 | 13.4 ± 10.0 |
| **Ca** | 109.2 ± 109.1 | 7.0 ± 9.2* |
| **Ti** | – | – |
| **Fe** | 7.3 ± 4.0 | 0.3 ± 0.6* |
| **Zn** | 1.6 ± 0.7 | 0.0 ± 0.0* |
| **F** | 178.2 ± 302.4 | 195.1 ± 136.3 |

* indicates elements whose peaks underwent a significant quantitative decrease in intensity after irradiation.

**Table S4.** X-ray diffraction peak count rate for 10 minerals after (A) compared to before (B) KrF irradiation.

| Filters | | 2Θ | Counts | | Mineral peak after compared to before laser irradiation | | | | | | | | | |
|---|---|---|---|---|---|---|---|---|---|---|---|---|---|---|
| Code | Type | | B-KrF | A-KrF | **Kao** | **Cli** | **Phi** | **Ill** | **Mas** | **Kok** | **Qua** | **Bei** | **Rut** | **Gyp** |
| F-25 | Q | 26.76 | 112 | 102 | PIR* | PIR* | PIR* | PP | PIR* | PP | PIR* | PIR* | PIR* | PIR* |
| F-30 | Q | 29.53-29.55 | 99 | 88 | PIR* | PIR* | PIR* | PIR* | PIR* | PP | PIR* | PP | PIR* | PIR* |
| F-21 | Q | 11.65-11.70 | 68 | 33 | PIR* | PIR* | PIR* | PIR* | PIR* | PIR* | PIR* | PIR* | PIR* | PP |
| F-33 | Q | 21.11-21.75 | 108 | 92 | PIR* | PIR* | PP | PIR* | PIR* | PP | PIR* | PIR* | PIR* | PIR* |
| F-34 | Q | 23.41 | 97 | – | PP | PD* | PD* | PP | PD* | PD* | PD* | PD* | PD* | PP |
| F-10 | Q | 26.72 | 115 | – | PD* | PD* | PD* | PP | PD* | PP | PP | PD* | PP | PD* |
| F-43 | Q | 5.72 | 10 | – | PD* | PP | PD* | PD* | PD* | PD* | PD* | PP | PD* | PD* |
| F-61 | Q | 32.92 | 74 | – | PD* | PD* | PP | PD* | PD* | PD* | PD* | PD* | PD* | PP |
| F-48 | Q | 36.18-36.31 | 87 | 84 | PP | PIR* | PP | PP | PIR* | PP | PP | PIR* | PP | PP |
| F-11 | Q | 11.69 | 52 | – | PD* | PD* | PD* | PD* | PD* | PD* | PD* | PD* | PD* | PP |
| F-56 | Q | 20.82 | 117 | – | PP | PP | PP | PP | PD* | PD* | PP | PD* | PD* | PP |
| F-54 | Q | 22.88 | 157 | – | PD* | PP | PP | PP | PD* | PD* | PD* | PD* | PD* | PP |
| F-17 | T | 9.05 | 104 | – | PD* | PD* | PD* | PP | PD* | PD* | PD* | PD* | PD* | PD* |
| F-20 | T | 15.33 | 121 | – | PD* | PD* | PD* | PD* | PD* | PD* | PD* | PD* | PD* | PD* |
| F-6 | T | 18.14-18.17 | 3201 | 3035 | PIR* | PIR* | PIR* | PIR* | PIR* | PIR* | PIR* | PIR* | PIR* | PIR* |
| F-9 | T | 27.23 | 107 | – | PD* | PD* | PP | PD* | PD* | PD* | PP | PD* | PP | PD* |
| F-14 | T | 8.99 | 55 | – | PD* | PD* | PD* | PP | PD* | PD* | PD* | PD* | PD* | PD* |
| F-18 | T | 56.47 | 100 | – | PP | PP | PD* | PP | PD* | PD* | PD* | PD* | PP | PD* |

Q: quartz; T: Teflon; PD: Peak deletion; PIR: Peak intensity reduction; PP: Peak presence (without any change); Kao: kaolinite, Cli: clinochlore; Phi: phillipsite; Ill: illite; Mas: mascagnite; Kok: koktaite; Qua: quartz; Bei: beidellite; Rut: rutile; Gyp: gypsum. * indicates minerals whose peaks either completely disappeared or underwent a significant quantitative decrease in intensity after irradiation.

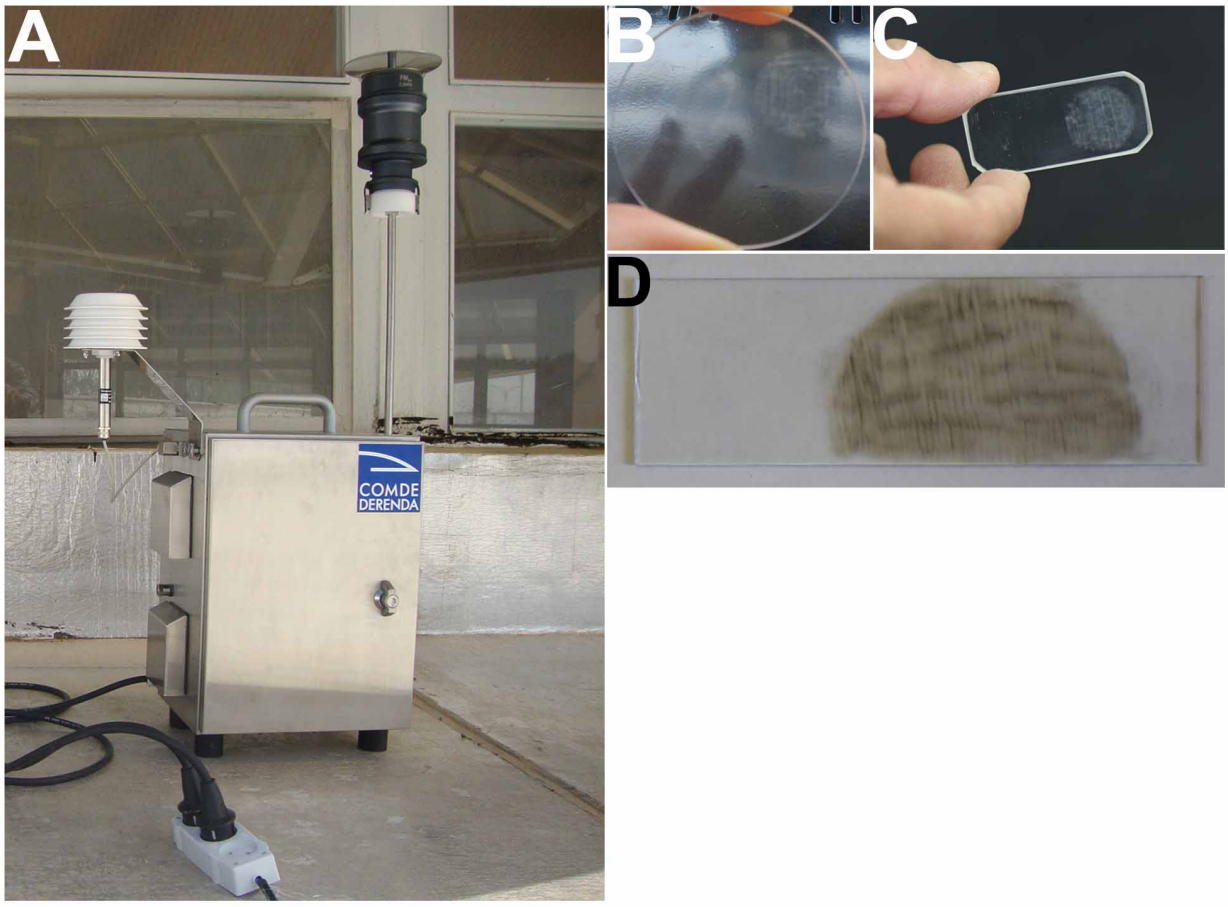


**Fig. S1.** Particulate matter (PM) collector and examples of detached and collected PM. (A) Medium Volume Sampler equipped with a $PM_{10}$ (PM < 10 μm) inlet. (B-D) PM that were detached from the filter and deposited onto glass plates (the round area on the upper right of B, right side of C and "dirty" half-circle on D).

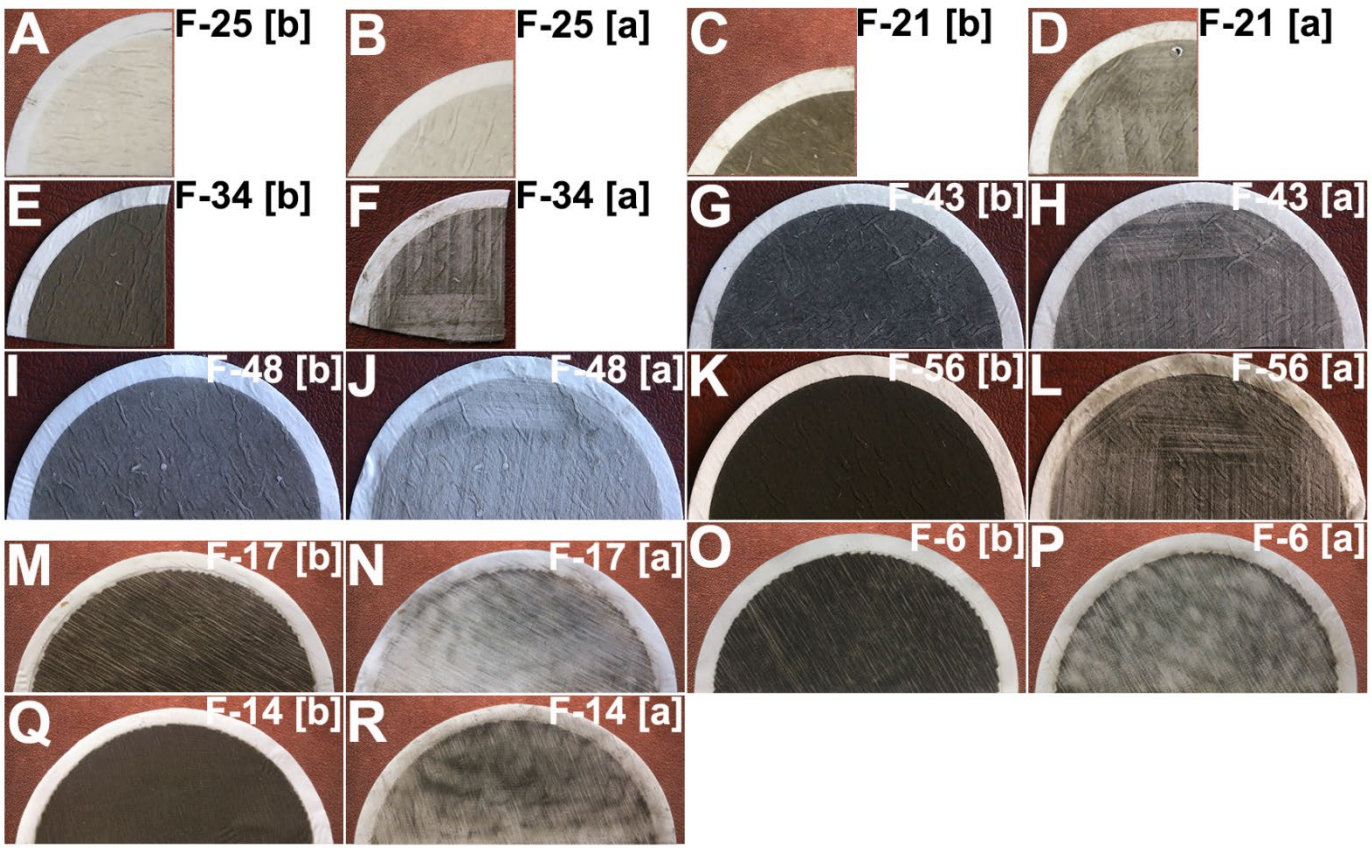


**Fig. S2.** PM-coated filters before [b] and after [a] KrF laser irradiation. Photographs are of quartz filters (before [A, C, E, G, I, and K] and after [B, D, F, H, J, and L] laser irradiation) and Teflon filters (before [M, O, and Q] and after laser irradiation [N, P, and R]). See Tables 1 and S1 for the filter code identities.

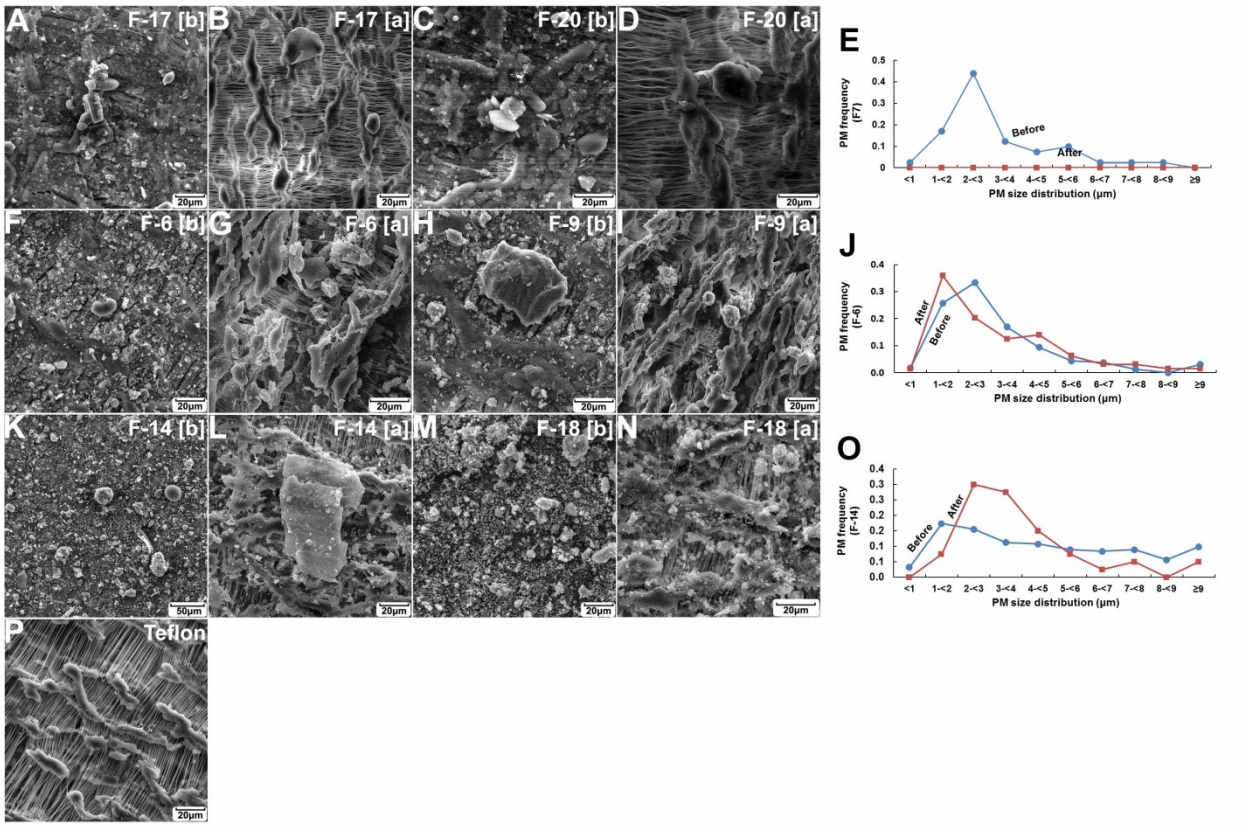


**Fig. S3.** SEM images of PM-coated Teflon filters before (A through M indicated by [b]) and after (B through N indicated by [a]) KrF laser irradiation. P is a non-PM exposed Teflon filter. Figures in the right hand column show the size distribution of PM collected on the filters. See Table S1 for the filter identities.

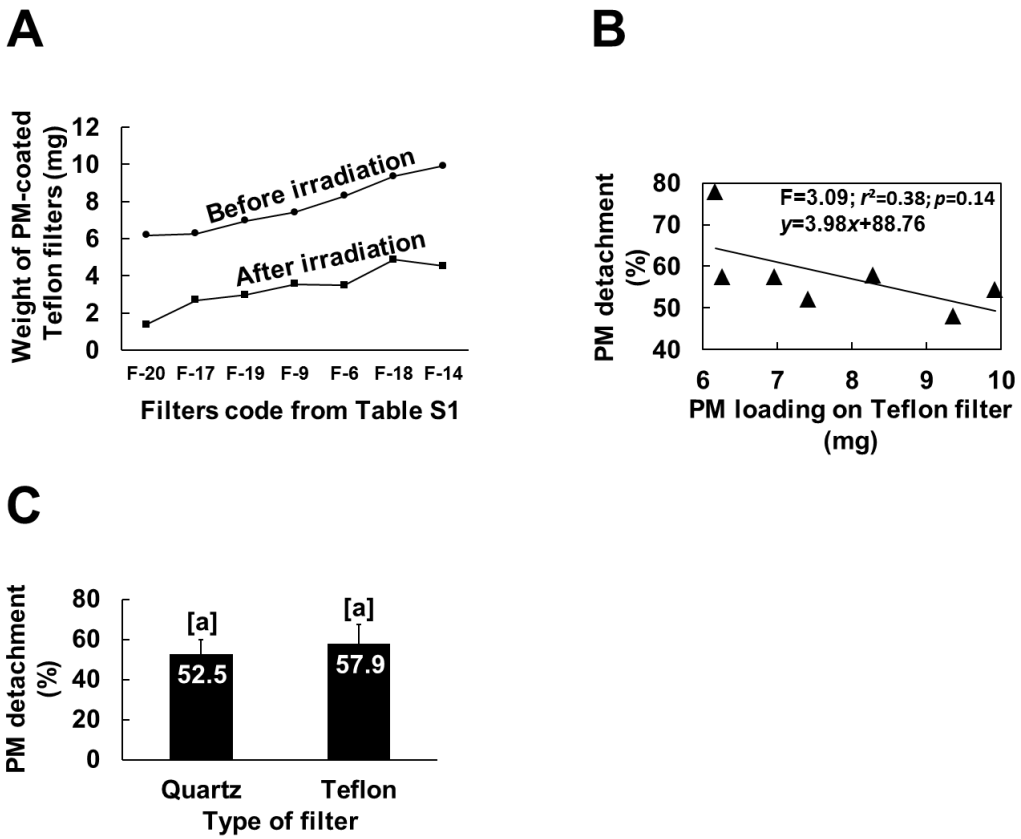


**Fig. S4.** Weight of seven PM-coated Teflon filters and PM detachment efficiency. (A) Weight of PM-coated Teflon filters before and after laser irradiation. (B) PM mass deposited on filters in relation to PM detachment efficiency. (C) Type of filter (quartz or Teflon) in relation to PM detachment efficiency. See Table S1 for the filter code identities.

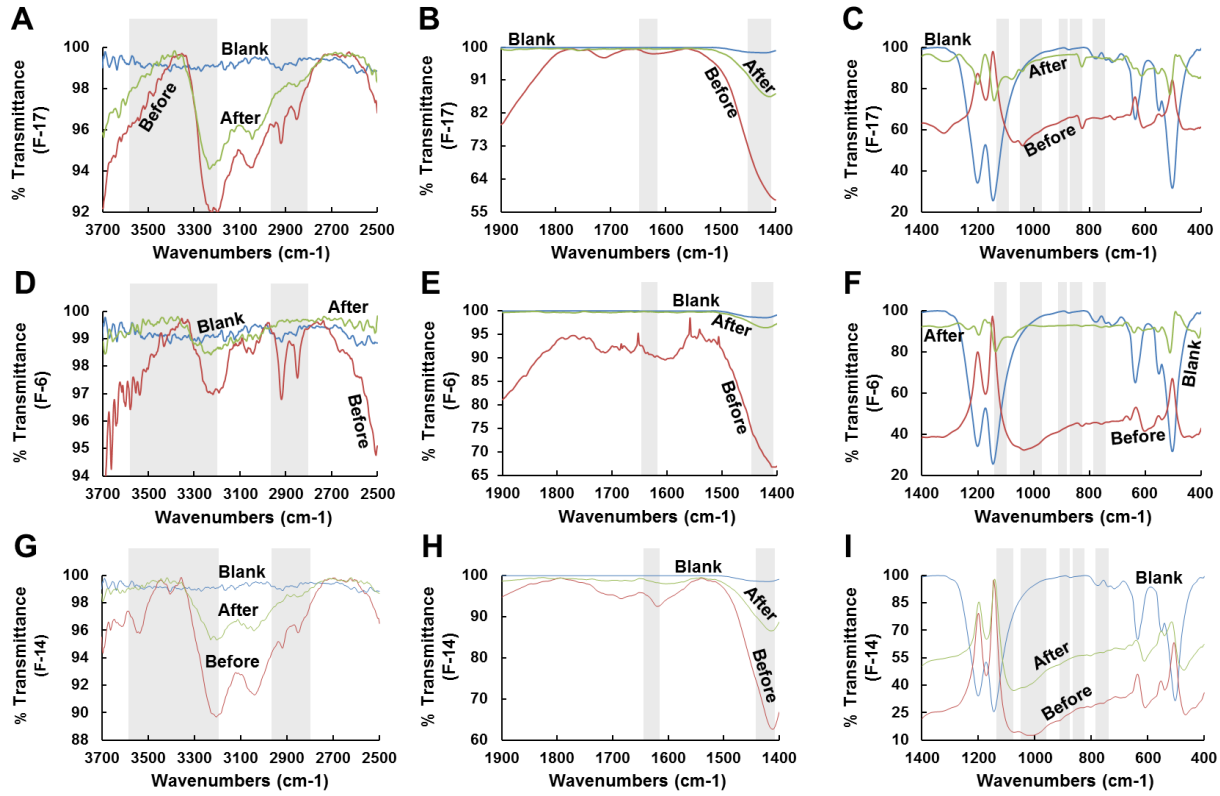


**Fig. S5.** ATR-FTIR of PM-coated Teflon filters before and after KrF laser irradiation. See Table S1 for the filter code identities.

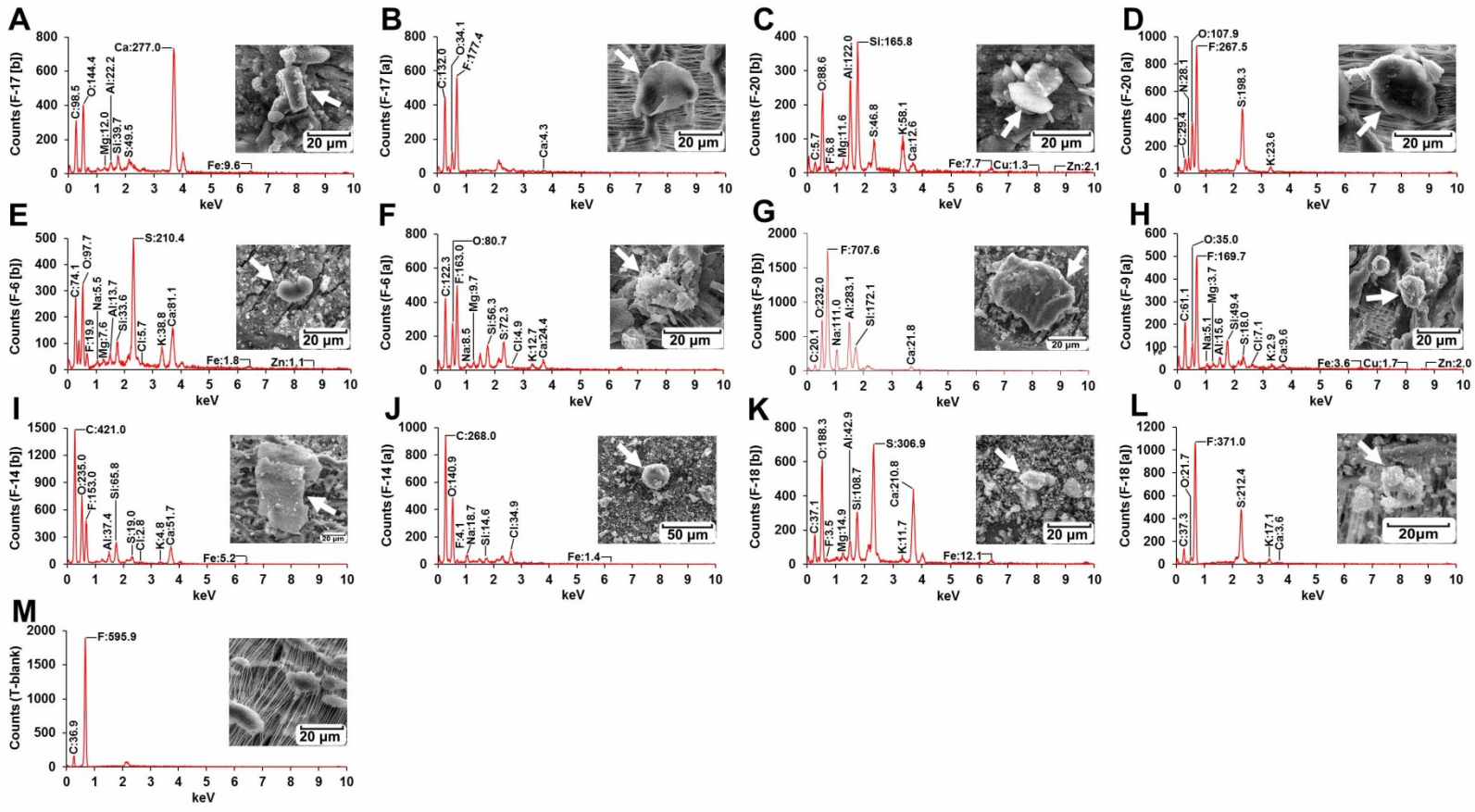


**Fig. S6.** EDS of PM-coated Teflon filters before and after KrF laser irradiation and blank (M). The inserted images show a field of view with the particle of interest. [b]: before laser irradiation; [a]: after laser irradiation. The white arrows point out analyzed particles. See Table S1 for the filter identities.